GEOPHYSICAL RESEARCH LETTERS, VOLUME 20, NUMBER 13, PAGES 1387-1390, JULY 9, 1993

LABORATORY ASSESSMENT OF THE EQUIVALENT APERTURES OF A ROCK FRACTURE

Andrew R. Piggott

National Water Research Institute, Burlington, Ontario

Derek Elsworth

Department of Mineral Engineering, Pennsylvania State University, University Park

Abstract. Hydraulic, electrical, and tracer test results are presented for a natural fracture in granite. The hydraulic and electrical apertures of the fracture are similar and suggest minimal fracture surface-to-surface contact. Tracer aperture exceeds hydraulic aperture indicating transport at a rate less than that predicted on the basis of hydraulic aperture. Numerical simulation of tracer transport reveals that transport within the fracture is not explicable in terms of parallel plate flow and that transport occurs locally at rates in excess of the overall rate defined by tracer aperture.

Introduction

This paper describes laboratory hydraulic, electrical, and tracer tests performed on a natural fracture in granite at two normal stress levels. Hydraulic and electrical test results are interpreted as equivalent hydraulic and electrical apertures where these terms denote the "cubic law aperture" of Tsang [1992] and the electrical analogue to this aperture. Conventional tracer test results are interpreted as equivalent tracer apertures, *viz* the "mass balance aperture" of Tsang [1992]. Composite conductivity tracer tests which measure the local rate of tracer transport further constrain the description of tracer transport. Comparison of the equivalent aperture magnitudes and numerical simulation of tracer transport for a parallel plate fracture are used to demonstrate the impact of variable aperture on transport.

Experimental Results and Analysis

The experiments were performed on a fracture oriented along the axis of a 190 mm diameter by 320 mm long core extracted from the Underground Research Laboratory of Atomic Energy of Canada Limited [Lang, 1986]. Tests were performed under nominally mated conditions at normal stresses of zero and 5 MPa.

Figure 1 illustrates the geometry of the specimen and the configuration of the inlet and outlet. The inlet and outlet were restricted to 60 mm of the 190 mm width of the fracture to limit the tracer dispersion contributed by these volumes. Analysis of tracer breakthrough at the inlet indicates that breakthrough may be explained by dispersed flow through a circular pipe representing the tubing connecting the tracer reservoir to the inlet. It is therefore assumed that the inlet itself does not contribute to dispersion. It is further assumed that the outlet does not contribute to dispersion since it is upstream of the outlet tubing section.

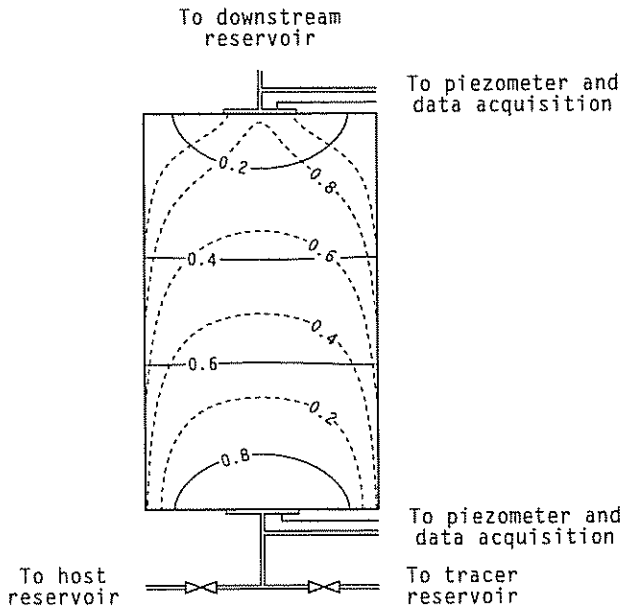

Fig. 1. Illustration of the fracture specimen showing the distributions of hydraulic head (solid) and tracer transit time (dashed) for a parallel plate fracture.

Also shown in Figure 1 are the distributions of hydraulic head and tracer transit time for a parallel plate fracture. Hydraulic head is normalized with respect to inlet and outlet values and transit time is expressed as the number of pore volumes at tracer breakthrough. The distributions were determined using a finite difference model of flow [Huyakorn and Pinder, 1983] and fluid particle tracking [Goode, 1990]. Tracer transit time was determined using the average of the parabolic velocity variation implied by parallel plate flow. Thus, transit time reflects only the geometric dispersion imparted by the configuration of the inlet and outlet.

Hydraulic Tests

The hydraulic apertures of the fracture were determined by measuring the rate of fluid flow through the specimen as a function of the hydraulic head loss between the inlet and outlet. Flow rates corresponding to several values of head loss were measured and linear regression was used to determine the average variation of flow rate with head loss [Piggott and

Paper number 93GL01384
0094-8534/93/93GL-01384$03.00

Elsworth, 1990]. Hydraulic apertures of 0.325 and 0.111 mm were determined at the zero and 5 MPa stress levels using

$$b_h = \sqrt[3]{\frac{12\nu}{g}\frac{L}{W\Gamma}\frac{\Delta Q}{\Delta h}} \quad (1)$$

where ν is the kinematic viscosity of the fluid, g is gravitational acceleration, L and W are the length and width of the fracture, Γ is a tortuosity factor which represents the constriction imposed by the inlet and outlet, and $\Delta Q/\Delta h$ is the slope of the linear regression model fit to the flow rate and head loss data. A value of $\Gamma = 0.7665$ was determined as the ratio of discharges computed with and without restriction of the width of the inlet and outlet.

Electrical Tests

The electrical apertures of the fracture were determined by measuring the conductance of the specimen as a function of the electrical conductivity of the saturating fluid. The intact portion of the specimen is essentially nonconductive and the conductance of the specimen is equal to that of the fracture. Electrical conductances corresponding to several fluid electrical conductivities were measured and linear regression was applied to determine the average variation of conductance with electrical conductivity [Piggott and Elsworth, 1990]. Electrical apertures of 0.336 and 0.114 mm were derived at the two stress levels using

$$b_e = \frac{L}{W\Gamma}\frac{\Delta G}{\Delta k_e} \quad (2)$$

where $\Delta G/\Delta k_e$ is the slope of the linear regression model fit to the electrical conductance and conductivity data.

Conventional Tracer Tests

Conventional tracer tests were performed by displacing a dilute sodium chloride host solution with a higher concentration tracer solution. Tracer concentrations at the inlet and outlet were determined by measuring the electrical conductivities of the fluid using integral flow-through conductivity cells and a data acquisition system [Piggott and Elsworth, 1990]. The relation between electrical conductivity and solute concentration was then used to determine concentration from electrical conductivity [Piggott, 1990]. Solute concentration was normalized with respect to initial and final values and time was translated into dimensionless form as the ratio of the cumulative volume of tracer solution injected to the integral mean volume computed from the breakthrough curve [Robinson and Tester, 1984].

The conventional tracer tests were simulated for a parallel plate fracture using an approach which represents inlet dispersion due to the variation of velocity across the diameter of the inlet tubing, velocity dispersion due to the variation of velocity across the width of the fracture implied in parallel plate flow, and geometric dispersion resulting from the varied motion of tracer within the plane of the fracture apparent in Figure 1. This approach assumes that a fluid particle travels along an arbitrary streamline within the inlet and then along a second streamline within the fracture where there is no correlation between the two streamlines. Streamlines are selected such that each represents an equal portion of the total discharge through the specimen. Total transit time is the sum of inlet and fracture transit times and the spectrum of the total transit times defines tracer breakthrough.

Inlet transit time is the product of mean inlet transit time and an inlet dispersion factor. Mean inlet transit time was obtained from the integral mean volume computed from the inlet breakthrough curve. Inlet dispersion factors were derived from the velocity variation across a circular pipe [Roberson and Crowe, 1980]. Fracture transit time is the product of mean fracture transit time and velocity and geometric dispersion factors. Mean fracture transit time was obtained from the integral mean volume computed from the outlet breakthrough curve less the integral mean volume for the inlet. Velocity dispersion factors were derived from the parabolic variation of flow velocity between parallel plates [Roberson and Crowe, 1980]. Geometric dispersion factors were obtained by simulating fluid particle transport between the inlet and outlet.

Figure 2 compares the conventional tracer test results to the simulated results. Normalized concentration, C_n, and the derivative of normalized concentration with dimensionless time, c_n, are shown as a function of dimensionless time, t_d. Note that the derivative accentuates the features of tracer breakthrough. The integral mean volumes of the inlet and specimen at zero and 5 MPa are 4.75 and 5.19 ml and 29.4 and 23.7 ml. Deducting the inlet volumes from the specimen volumes yields fracture volumes of 24.7 and 18.5 ml which translate to tracer apertures of 0.406 and 0.304 mm.

Two sets of simulated results are shown in Figure 2. In

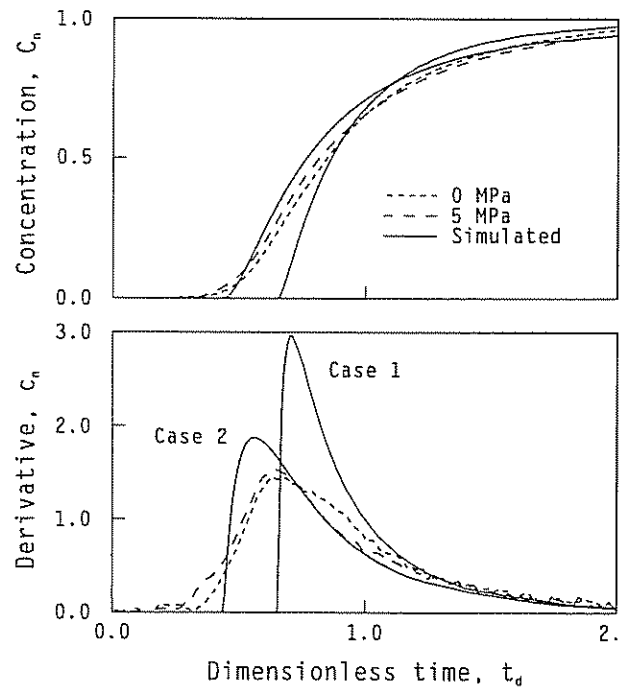

Fig. 2. Measured conventional tracer test results and simulated results for a parallel plate fracture without (Case 1) and with (Case 2) velocity dispersion.

Case 1, tracer transport occurs at the average of the velocity variation implied by parallel plate flow and only inlet and geometric dispersion are represented. In Case 2, all three dispersion mechanisms are represented. These two scenarios illustrate the magnitude of the potential contribution of velocity dispersion to the tracer test results.

Composite Conductivity Tracer Tests

Composite conductivity tracer tests were performed by displacing a dilute sodium chloride host solution with a tracer solution of higher concentration following the procedure applied to porous media by Rehbinder [1978]. This results in a decrease in the resistance of the specimen as the tracer traverses the fracture. The resistance of the specimen was measured between the inlet and outlet and normalized with respect to initial and final values.

Simulation of the composite conductivity tracer tests was performed for a parallel plate fracture using the finite difference model of flow with a spatially and temporally varying electrical transmissivity distribution which represents the motion and dispersion of the tracer. Mean transit times at each node were determined using the particle tracking algorithm. Next, the electrical transmissivity at each node was obtained by integrating electrical conductivity over the width of the fracture. The electrical conductivity at a position within the cross-section is equal to the electrical conductivity at the inlet at the time at which the fluid at that position entered the fracture. This time is constant over the cross-section without velocity dispersion and variable with velocity dispersion. Electrical conductivity at the inlet was modeled assuming flow through a circular pipe. The discharge through the fracture was computed from the transmissivity distribution and normalized with respect to initial and final values.

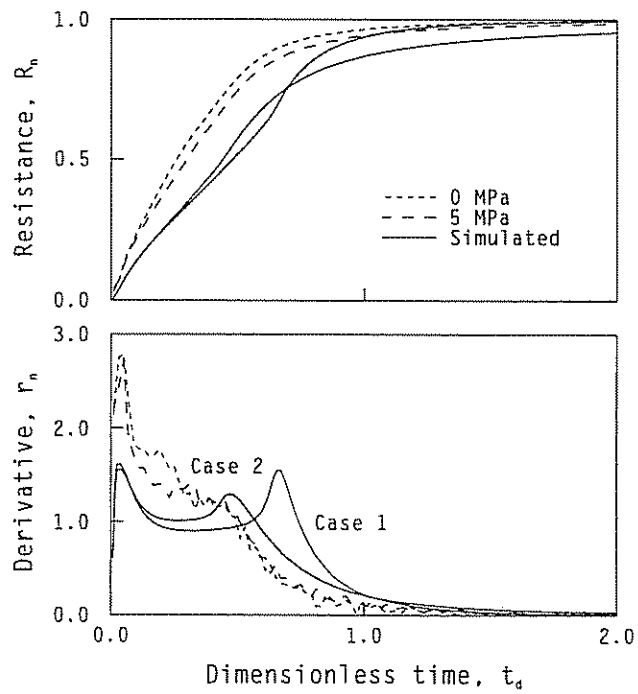

Fig. 3. Measured composite conductivity tracer test results and simulated results for a parallel plate fracture without (Case 1) and with (Case 2) velocity dispersion.

Figure 3 compares the measured and simulated values of normalized resistance, R_n, and the derivative of normalized resistance with dimensionless time, r_n, as a function of dimensionless time. Since resistance is indicative of the penetration of the tracer, the derivative illustrates the local rate of tracer transport. The simulated results display four characteristic stages. Transport occurs initially at a greater-than-average rate as the result of divergent flow in the vicinity of the inlet. Transport then slows to a near constant rate as the tracer traverses the central portion of the fracture. Accelerated transport occurs as the result of convergent flow in the vicinity of the outlet. The protracted tail is indicative of dispersed transport.

Discussion and Conclusions

Table 1 lists the equivalent apertures at the two stress levels and compares the change in these apertures to the closure of the fracture measured using displacement pins fixed to the ends of the specimen. Closure was nonuniform and was accompanied by a shear displacement of 0.093 mm.

Variable aperture and fracture surface-to-surface contact yield contrasting hydraulic and electrical apertures [Brown, 1989]. For flow through an obstructed and variably conductive domain, equivalent conductivity may be approximated as the product of a tortuosity factor and the geometric mean conductivity of the unobstructed portion of the domain [Piggott and Elsworth, 1992]. For a fracture, this approximation yields a hydraulic transmissivity of

$$T_h = \frac{g}{12\nu} b_h^3 \approx \frac{g}{12\nu} \tau \langle b^3 \rangle_g = \frac{g}{12\nu} \tau \langle b \rangle_g^3 \quad (3)$$

and an electrical transmissivity of

$$T_e = k_e b_e = k_e \tau \langle b \rangle_g . \quad (4)$$

Here, τ is a tortuosity factor regulated by the extent of surface-to-surface contact and $\langle b \rangle_g$ is the geometric mean aperture of the open portion of the fracture where it can be shown that $\langle b^3 \rangle_g = \langle b \rangle_g^3$. The ratio of the hydraulic and electrical apertures derived from (3) and (4) is

$$\frac{b_e}{b_h} = \frac{\tau \langle b \rangle_g}{\sqrt[3]{\tau \langle b \rangle_g^3}} = \tau^{2/3} \quad (5)$$

which implies that the discrepancy between hydraulic and electrical aperture is a function of the tortuosity imposed by surface-to-surface contact. The tortuosity factor decreases

Table 1. Summary of Equivalent Apertures

Test Type	Equivalent Aperture (mm)		
	0 MPa	5 MPa	Change
Hydraulic	0.325	0.111	0.214
Electrical	0.336	0.114	0.222
Tracer	0.406	0.304	0.102
Closure			0.312

from unity as contact area increases from zero and therefore electrical aperture is less than or equal to hydraulic aperture. This is confirmed by computational studies of variable aperture fractures [Brown, 1989] and a laboratory study of an obstructed fracture which illustrates contrasting hydraulic and electrical apertures in the absence of variable aperture [Piggott, 1990]. The hydraulic and electrical apertures listed in Table 1 are effectively equal and imply minimal contact area at both stress levels. Minimal contact area requires that the mean aperture of the fracture is large, relative to the standard deviation of aperture.

The tracer apertures listed in Table 1 exceed the hydraulic apertures. This implies tracer transport at an overall rate less than that anticipated on the basis of hydraulic aperture. The change in hydraulic aperture between the two stress levels is larger than that in tracer aperture which, in turn, is less than the closure of the fracture. The contrast between these changes may result from the fact that hydraulic aperture reflects aperture constrictions whereas tracer aperture reflects average aperture. The discrepancy between the change in tracer aperture and fracture closure is not explained by this assertion since closure is a direct measure of the change in average aperture.

The tracer test results shown in Figures 2 and 3 display a limited change in dispersion between the two stress levels despite the significant change in aperture. Neither Case 1 nor 2 precisely replicate the measured data. The conventional results display greater dispersion at small times than predicted for parallel plate flow. The composite conductivity results reveal that, at small times, normalized resistance and its derivative are greater than the values predicted for parallel plate flow. These elevated values imply transport locally at rates in excess of that for parallel plate flow, a behaviour consistent with preferential tracer transport in aperture channels. Case 2, which includes velocity dispersion, better replicates the tracer test results and this may indicate that velocity dispersion is apparent in the measured data. However, velocity dispersion also emulates accelerated transport resulting from preferential flow in aperture channels and therefore the improved agreement is not sufficient to uniquely identify the dispersive mechanism.

The spatial variation of aperture within a fracture is difficult to obtain, particularly *in situ*, and characterization of transport must proceed on the basis of more measurable data. Hydraulic, electrical, and tracer test results as presented in this paper are examples of data which is measurable under a useful range of laboratory and *in situ* conditions. The discrepancies between equivalent apertures and between tracer test results and results predicted for parallel plate flow demonstrate the influence of variable aperture on transport without the encumbrance of determining the aperture distribution. The composite conductivity tracer test applied in this paper responds to tracer transport differently than the conventional form of tracer test and provides valuable additional constraint to the description of transport.

Acknowledgements. The fracture specimen was provided by Atomic Energy of Canada Limited. Instrumentation and testing of the specimen was supported by the U.S. National Science Foundation under award number MSM-8708976.

References

Brown, S.R., Transport of fluid and electric current through a single fracture, *J. Geophys. Res.*, 94, 9429-9438, 1989.

Goode, D.J., Particle velocity interpolation in block-centered finite difference groundwater flow models, *Water Resour. Res.*, 26, 925-940, 1990.

Huyakorn, P.S., and G.F. Pinder, *Computational Methods in Subsurface Flow*, 473 pp., Academic Press, Orlando, 1983.

Lang, P.A., Overview of the fracture testing program at the Underground Research Laboratory, *TR-408*, 17 pp., Atomic Energy of Canada Limited, Chalk River, 1986.

Piggott, A.R., Analytical and experimental studies of rock fracture hydraulics, Ph.D. thesis, 252 pp., Pennsylvania State Univ., University Park, August 1990.

Piggott, A.R., and D. Elsworth, Laboratory studies of transport within a single rock fracture, in *Proc. Int. Symp. Rock Joints*, edited by N. Barton and O. Stephansson, pp. 397-404, A.A. Balkema, Rotterdam, 1990.

Piggott, A.R., and D. Elsworth, Analytical relations for flow through obstructed domains, *J. Geophys. Res.*, 97, 2085-2093, 1992.

Rehbinder, G., Measurement of the average pore velocity of water flowing through a rock specimen, *Rock Mech.*, 11, 19-28, 1978.

Roberson, J.A., and C.T. Crowe, *Engineering Fluid Mechanics*, 661 pp., Houghton Mifflin, Boston, 1980.

Robinson, B.A., and J.W. Tester, Dispersed fluid flow in fractured reservoirs: An analysis of tracer-determined residence time distributions, *J. Geophys. Res.*, 89, 10374-10384, 1984.

Tsang, Y.W., Usage of "equivalent apertures" for rock fissures as derived from hydraulic and tracer tests, *Water Resour. Res.*, 28, 1451-1455, 1992.

D. Elsworth, Pennsylvania State University, 104 Mineral Sciences Building, University Park, PA 16802.

A. R. Piggott, National Water Research Institute, 867 Lakeshore Road, Burlington, Ontario, L7R 4A6.

(Received August 4, 1992;
revised March 24, 1993;
accepted May 24, 1993.)